

Oikos

Appendix oik-07512

Deshpande, J. N., Kaltz, O. and Fronhofer, E. A. 2020. Host-parasite dynamics set the ecological theatre for the evolution of state- and context-dependent dispersal in hosts. – Oikos doi: 10.1111/oik.07512

## Appendix 1

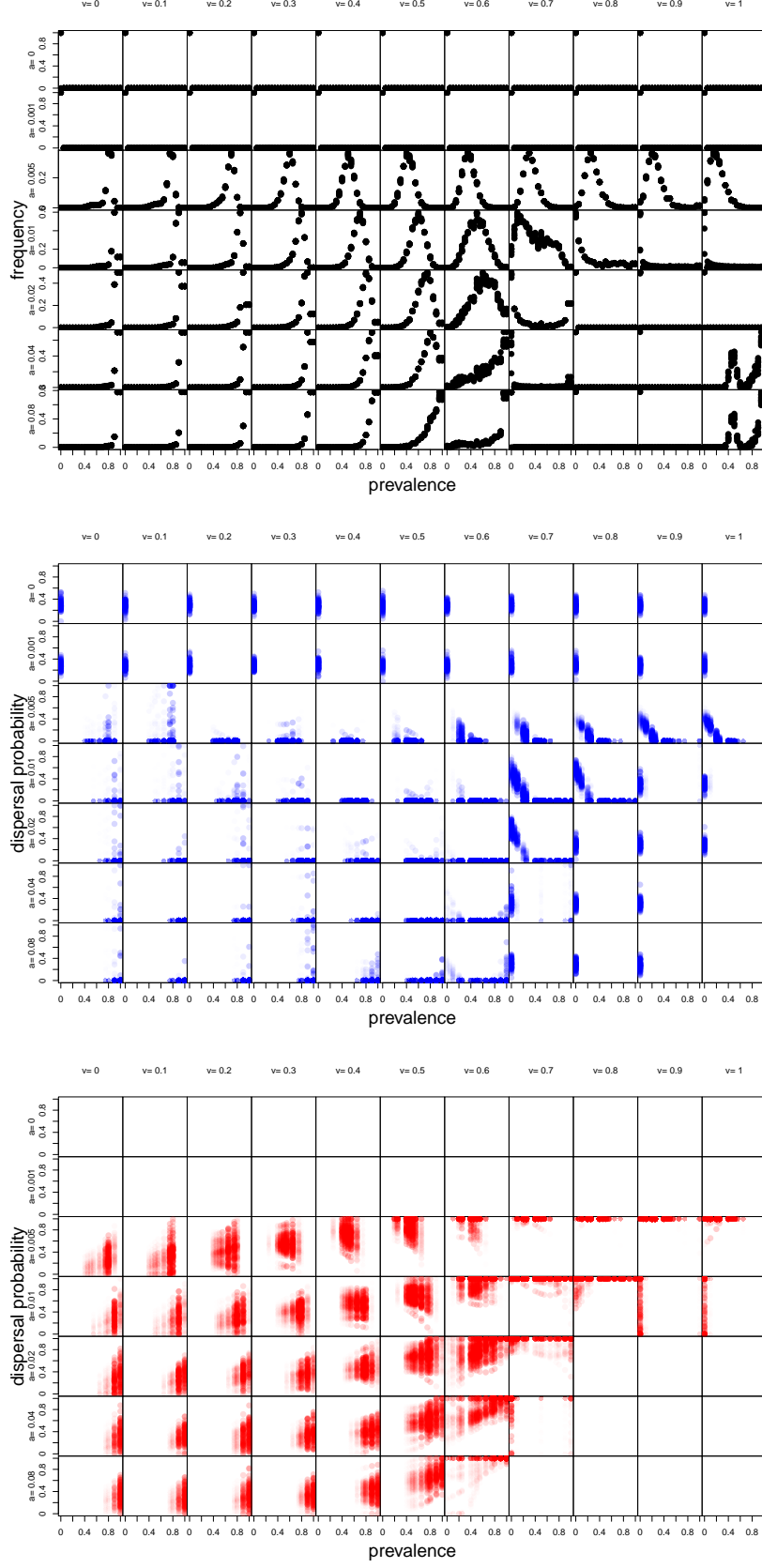


Figure A1. Effect of varying the searching efficiency of the parasite ( $a = 0, 0.001, 0.005, 0.01, 0.05, 0.08$ ; from top to bottom) as well as the virulence ( $v = 0, 0.1, \dots, 1$ ; from left to right) on the focal scenario ( $\lambda_0 = 4, \beta = 4, \mu = 0.1$ , and  $\varepsilon = 0.05$ ). Top (black): Histograms of local prevalences of all patches, over all time. Center (blue): Dispersal probability as a function of prevalence, if susceptible. Bottom (red): Dispersal probability as a function of prevalence, if infected.

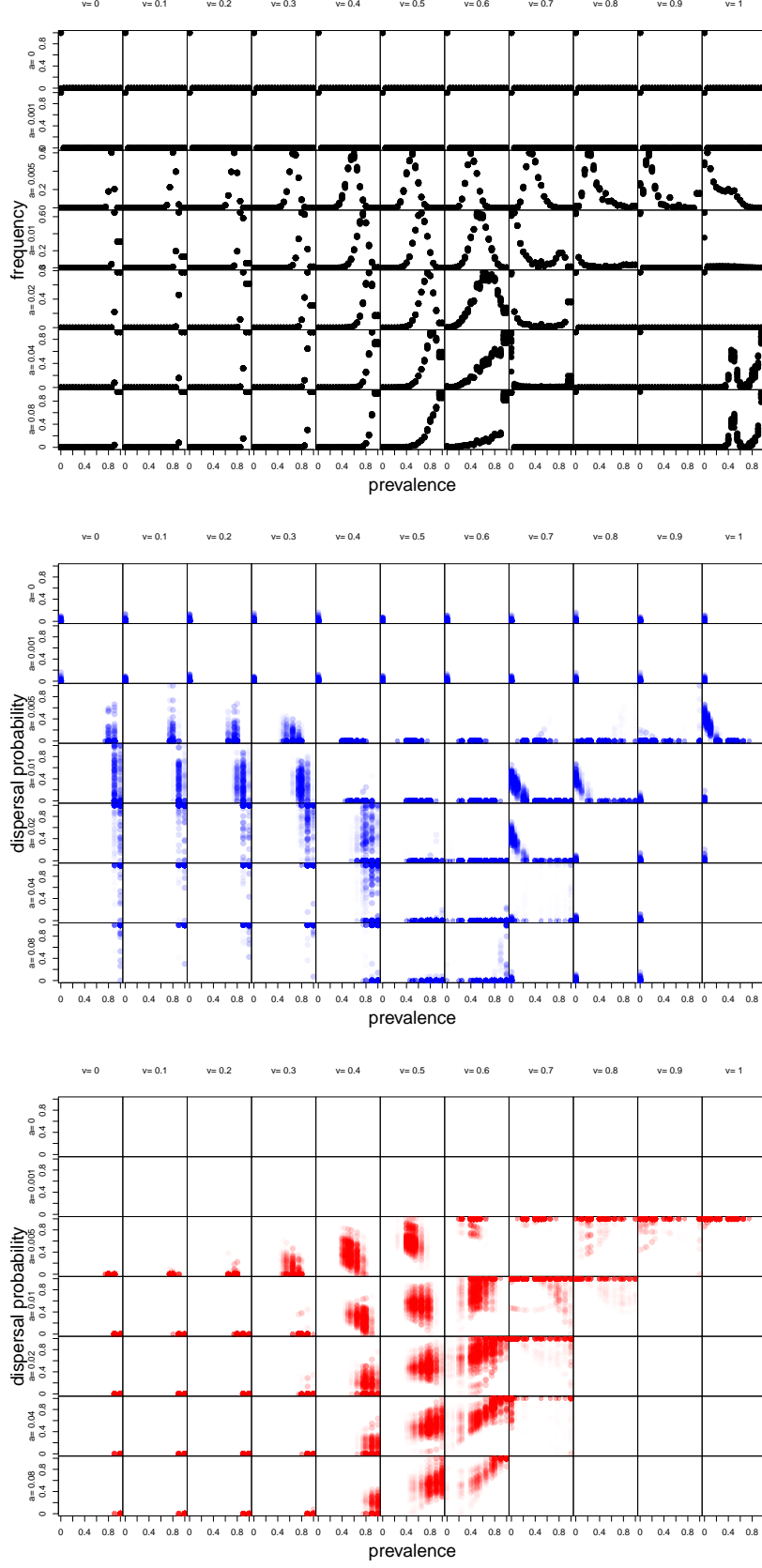


Figure A2. Effect changing local patch extinction risk (here set to  $\varepsilon = 0$ ) and of varying the searching efficiency of the parasite ( $a = 0, 0.001, 0.005, 0.01, 0.05, 0.08$ ; from top to bottom) as well as the virulence ( $v = 0, 0.1, \dots, 1$ ; from left to right) on the focal scenario ( $\lambda_0 = 4, \beta = 4, \mu = 0.1$ ). Top (black): Histograms of local prevalences of all patches, over all time. Center (blue): Dispersal probability as a function of prevalence, if susceptible. Bottom (red): Dispersal probability as a function of prevalence, if infected.

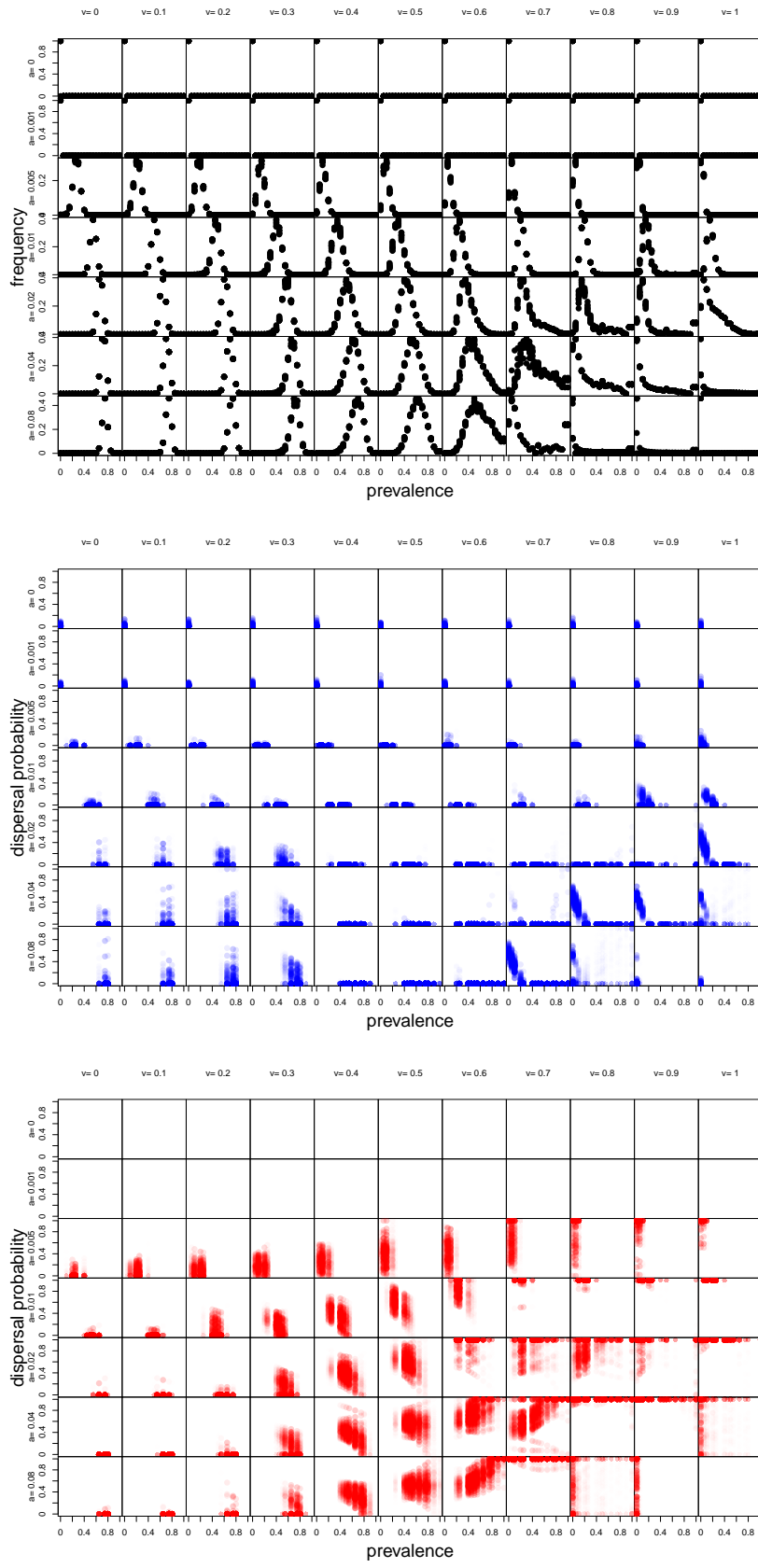


Figure A3. Effect changing transmission rate (here set to  $\beta = 2$ ) and of varying the searching efficiency of the parasite ( $a = 0, 0.001, 0.005, 0.01, 0.05, 0.08$ ; from top to bottom) as well as the virulence ( $v = 0, 0.1, \dots, 1$ ; from left to right) on the focal scenario ( $\lambda_0 = 4, \mu = 0.1, \varepsilon = 0$ ). Top (black): Histograms of local prevalences of all patches, over all time. Center (blue): Dispersal probability as a function of prevalence, if susceptible. Bottom (red): Dispersal probability as a function of prevalence, if infected.

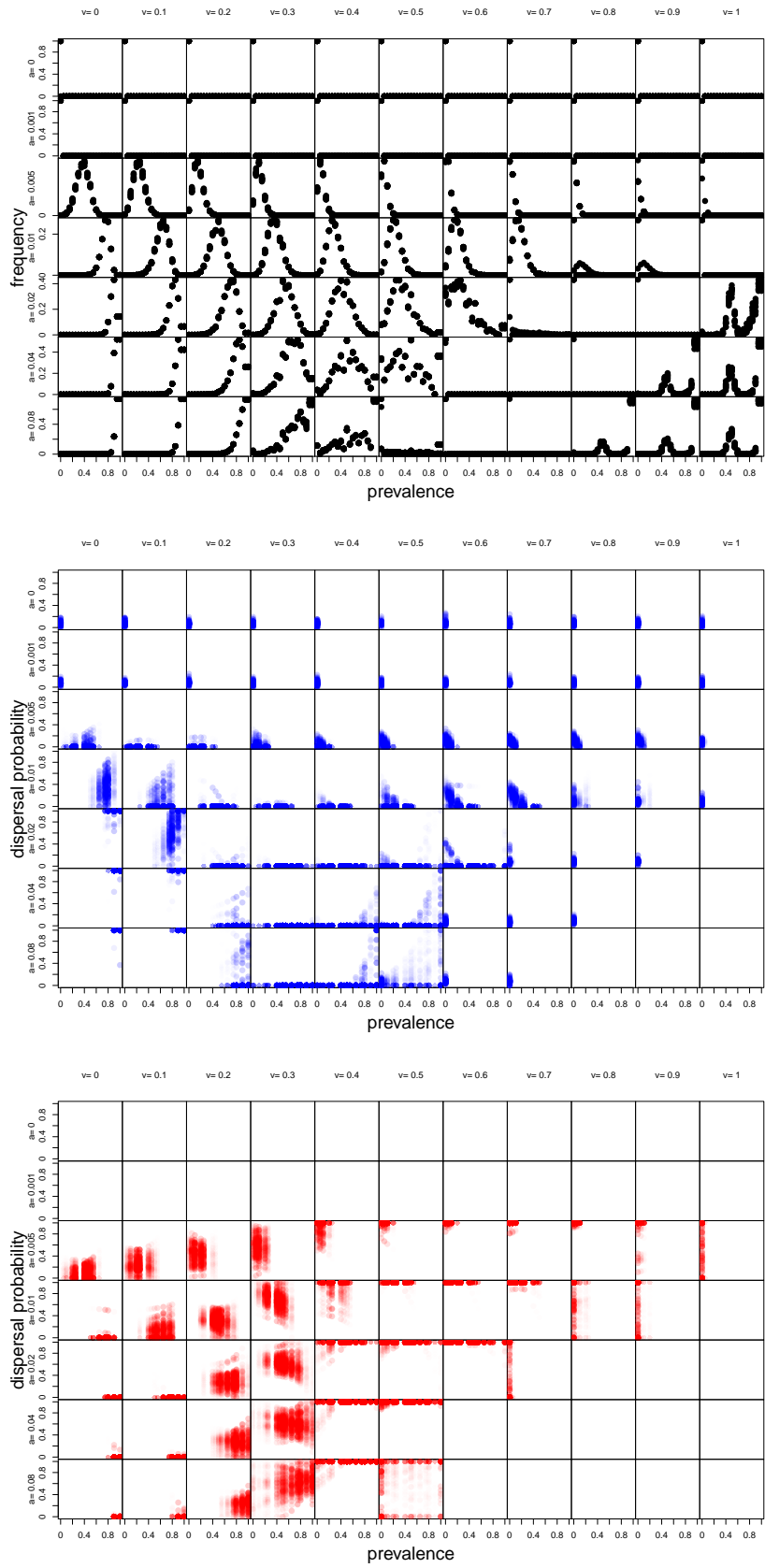


Figure A4. Effect changing fecundity (here set to  $\lambda = 2$ ) and of varying the searching efficiency of the parasite ( $a = 0, 0.001, 0.005, 0.01, 0.05, 0.08$ ; from top to bottom) as well as the virulence ( $v = 0, 0.1, \dots, 1$ ; from left to right) on the focal scenario ( $\beta = 4, \mu = 0.1, \varepsilon = 0$ ). Top (black): Histograms of local prevalences of all patches, over all time. Center (blue): Dispersal probability as a function of prevalence, if susceptible. Bottom (red): Dispersal probability as a function of prevalence, if infected.

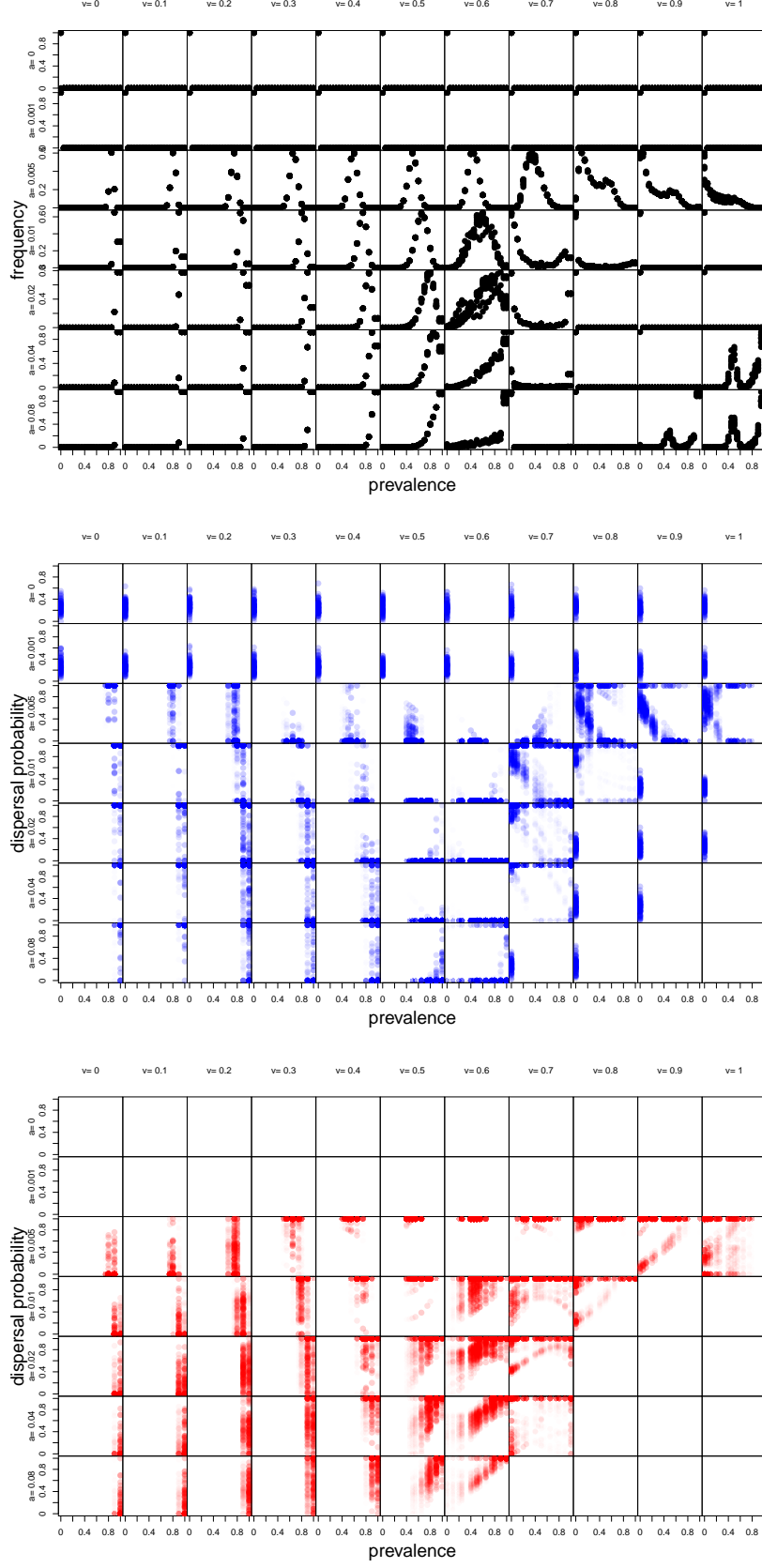


Figure A5. Effect reducing dispersal mortality (here set to  $\mu = 0.01$ ) and of varying the searching efficiency of the parasite ( $a = 0, 0.001, 0.005, 0.01, 0.05, 0.08$ ; from top to bottom) as well as the virulence ( $v = 0, 0.1, \dots, 1$ ; from left to right) on the focal scenario ( $\lambda_0 = 4, \beta = 4, \varepsilon = 0$ ). Top (black): Histograms of local prevalences of all patches, over all time. Center (blue): Dispersal probability as a function of prevalence, if susceptible. Bottom (red): Dispersal probability as a function of prevalence, if infected.

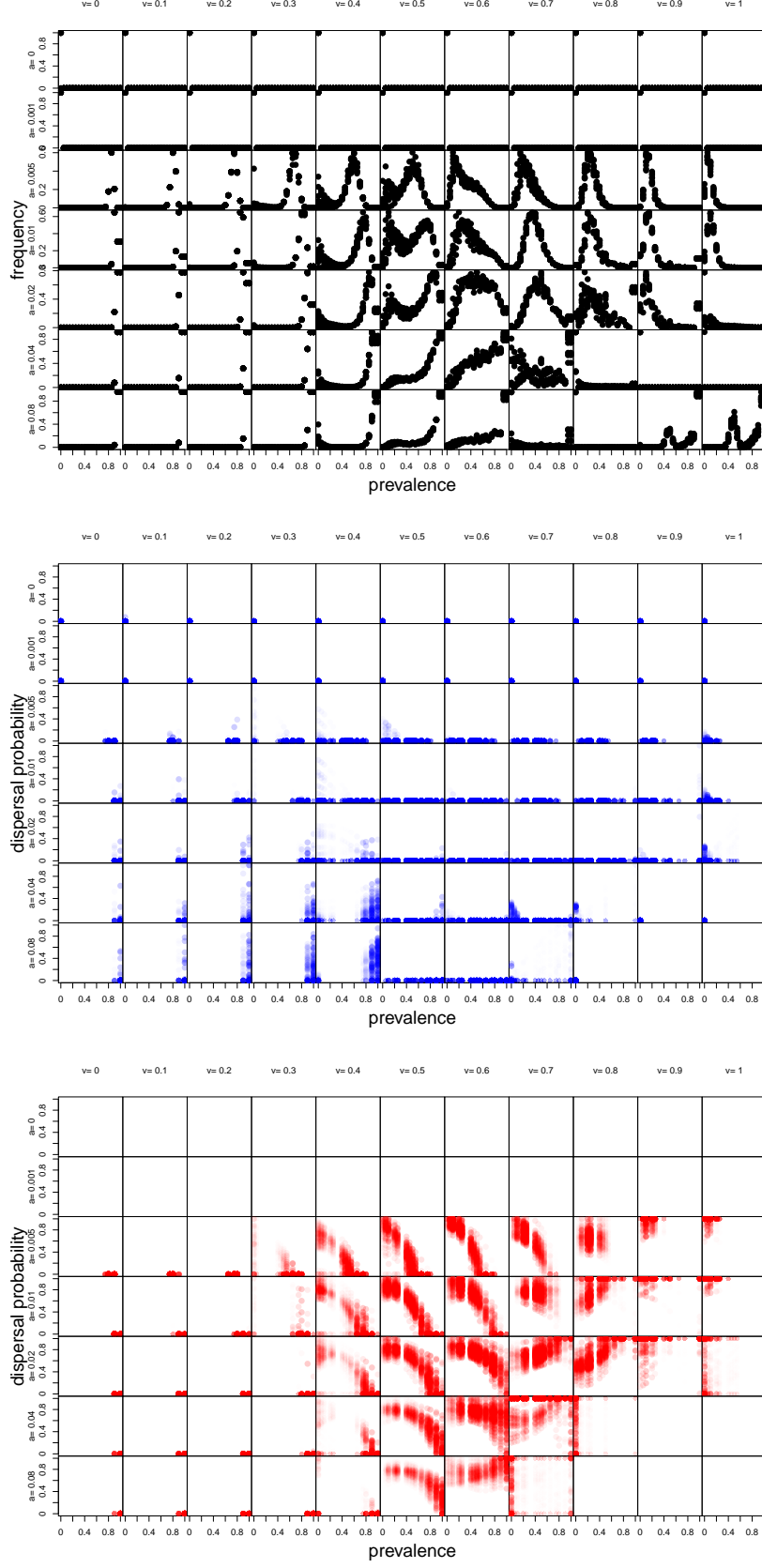


Figure A6. Effect increasing dispersal mortality (here set to  $\mu = 0.5$ ) and of varying the searching efficiency of the parasite ( $a = 0, 0.001, 0.005, 0.01, 0.05, 0.08$ ; from top to bottom) as well as the virulence ( $v = 0, 0.1, \dots, 1$ ; from left to right) on the focal scenario ( $\lambda_0 = 4, \beta = 4, \varepsilon = 0$ ). Top (black): Histograms of local prevalences of all patches, over all time. Center (blue): Dispersal probability as a function of prevalence, if susceptible. Bottom (red): Dispersal probability as a function of prevalence, if infected.

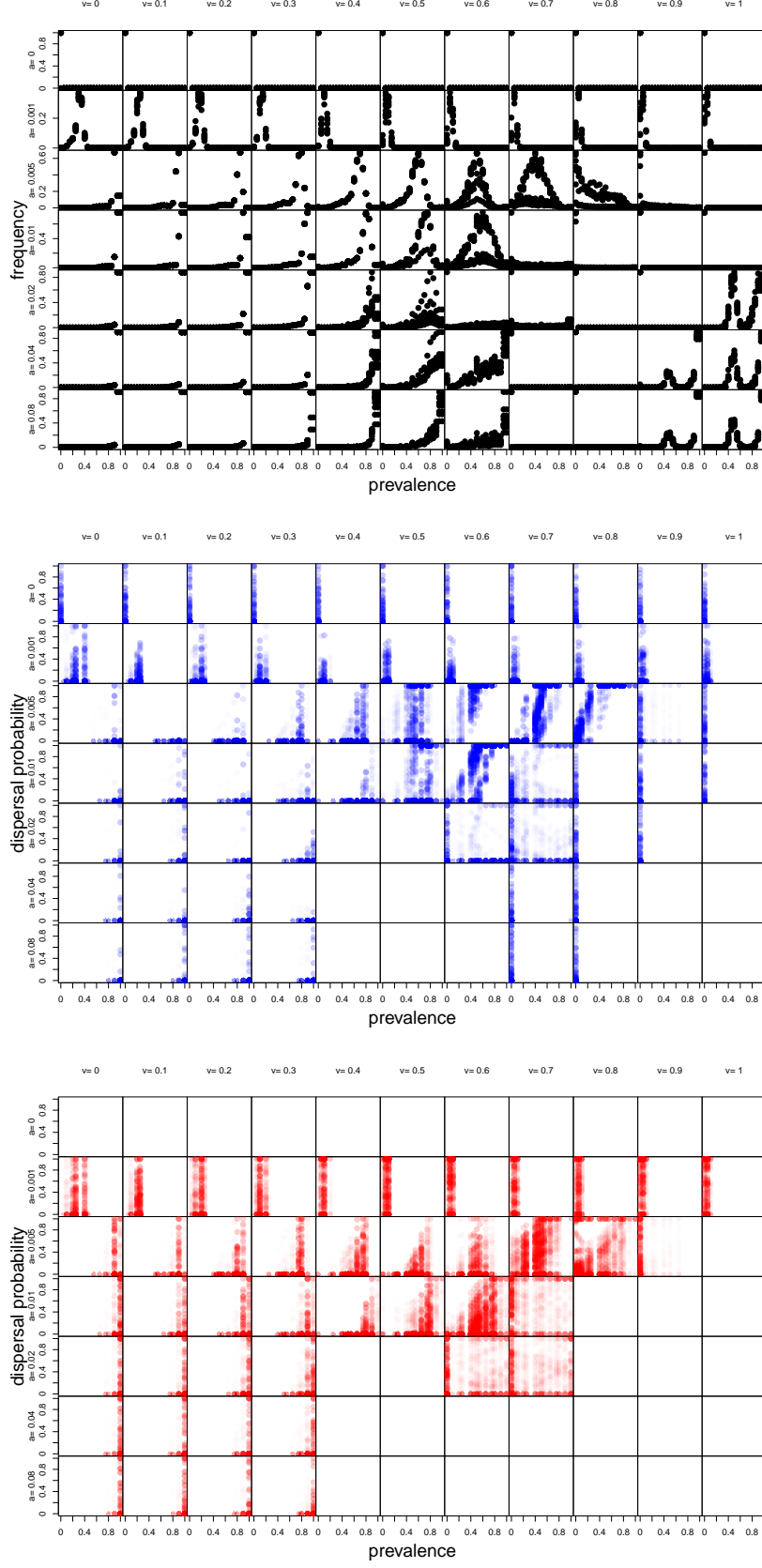


Figure A7. Focal scenario ( $\lambda_0 = 4$ ,  $\beta = 4$ ,  $\mu = 0.1$ , and  $\varepsilon = 0.05$ ) without kin competition and infection while varying the searching efficiency of the parasite ( $a = 0, 0.001, 0.005, 0.01, 0.05, 0.08$ ; from top to bottom) as well as the virulence ( $v = 0, 0.1, \dots, 1$ ; from left to right). Top (black): Histograms of local prevalences of all patches, over all time. Center (blue): Dispersal probability as a function of prevalence, if susceptible. Bottom (red): Dispersal probability as a function of prevalence, if infected.

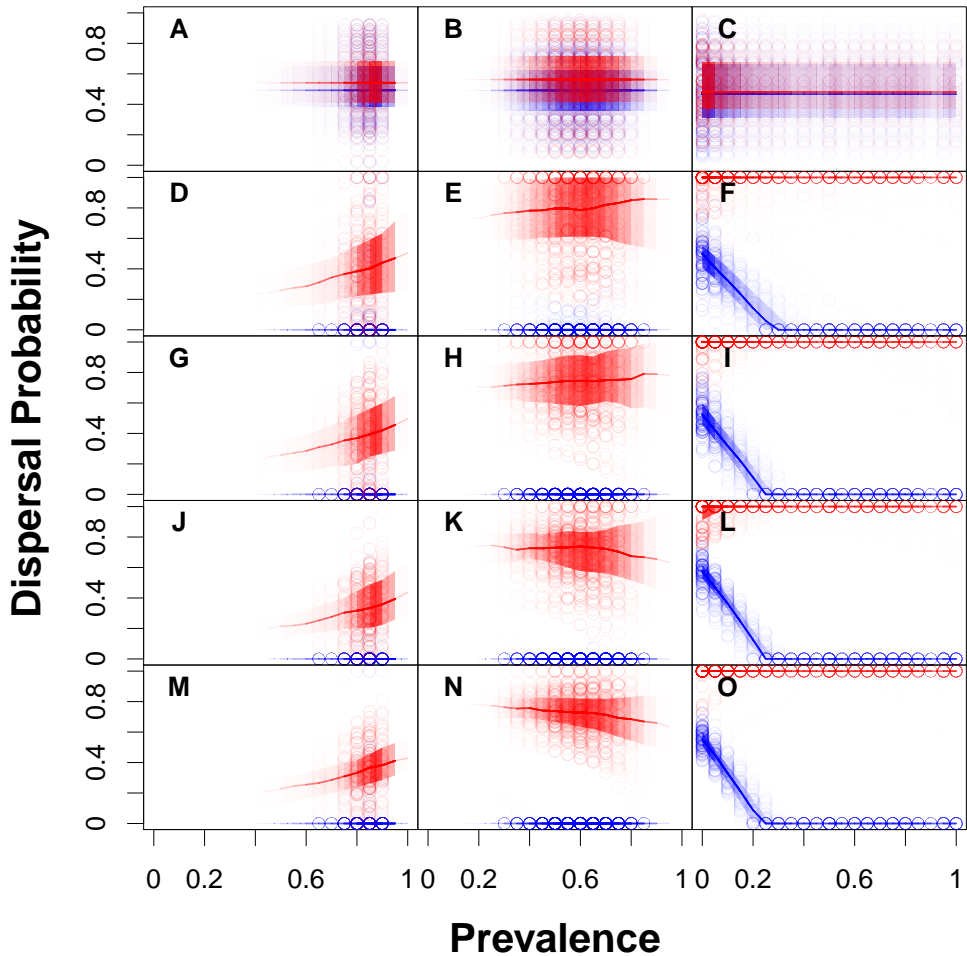


Figure S8: Measured dispersal reaction norms for prevalence- and infection state-dependent dispersal as in Fig. ?? for the standard scenario only. Rows show how the reaction norm shape changes through time (from top to bottom:  $t = 0$ ,  $t = 2500$ ,  $t = 5000$ ,  $t = 7500$ ,  $t = 9999$ ), illustrating that our standard simulation time (10000 generations) is sufficient to reach a steady state. Red colours represent reaction norms of infected individuals and blue colours show reaction norms when susceptible. Virulence increases from left to right.  $v = 0.2$  for A, D, G, J and M,  $v = 0.5$  for B, E, H, K and N, and  $v = 0.8$  for C, F, I, L and O. The lines represent the median dispersal probability corresponding to that prevalence and the shaded regions are the quartiles. Constant model parameters:  $\lambda_0 = 4$ ,  $\alpha = 0.01$ ,  $\beta = 4$ ,  $a = 0.01$ ,  $\mu = 0.1$ ,  $\epsilon = 0.05$ .

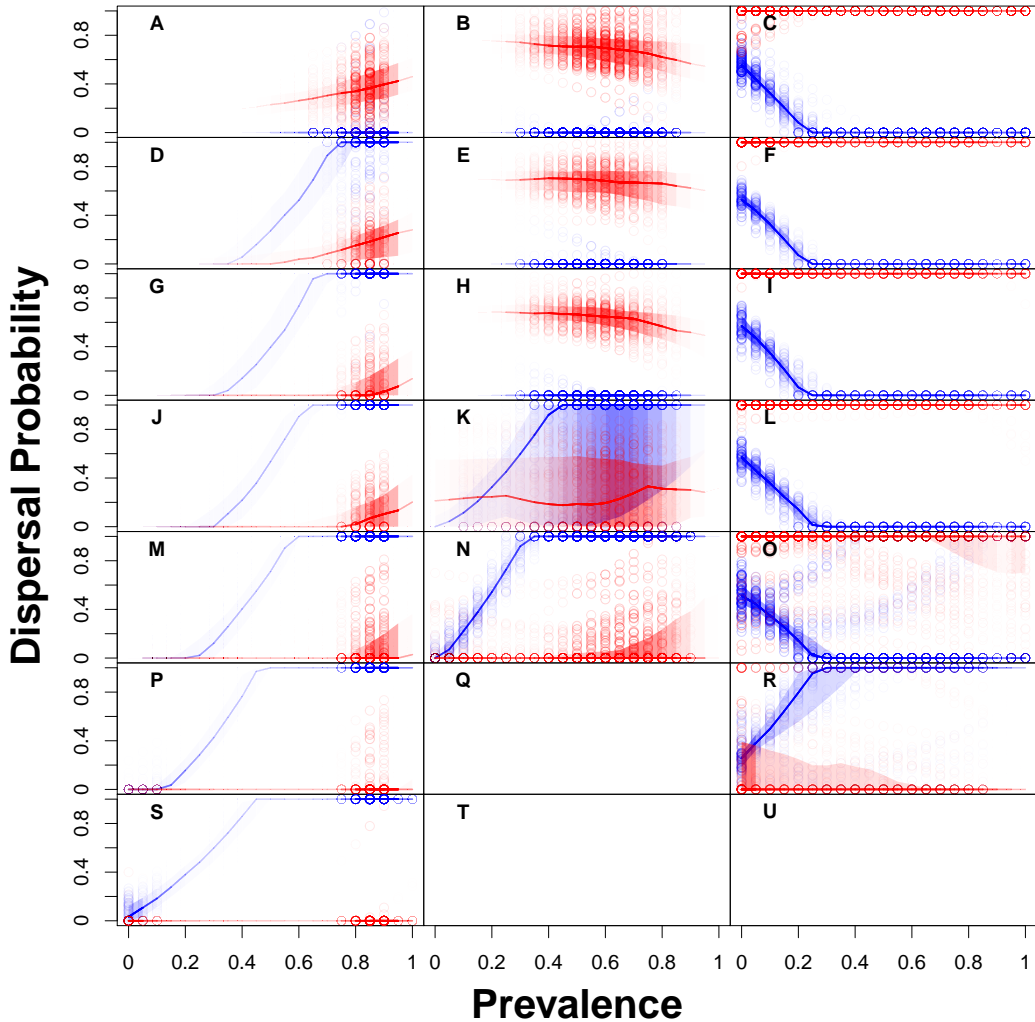


Figure S9: Evolutionarily stable dispersal reaction norms for prevalence- and infection state-dependent dispersal for differential dispersal costs of susceptible ( $\mu_{susceptible} = \text{const.} = 0.1$ ) and infected individuals (from top to bottom:  $\mu_{infected} = \{0.1, 0.12, 0.14, 0.16, 0.2, 0.3, 0.4\}$ ) and the standard scenario. Red colours represent reaction norms of infected individuals and blue colours show reaction norms when susceptible. Virulence increases from left to right.  $v = 0.2$  for A, D, G, J and M,  $v = 0.5$  for B, E, H, K and N, and  $v = 0.8$  for C, F, I, L and O. This graph shows the reaction norms of 100 randomly chosen individuals at the end of the simulation (points) weighted by the normalised frequency of prevalences across space and time, that is, darker shades correspond to higher frequency of prevalence and lighter to lower frequency across space and time. We chose this weighting because the ecological settings of the simulations dictate the prevalences that occur and therefore also whether selection can act on parts of the reaction norm. Our approach (weighting combined with total simulation time, see Fig. S8) therefore guarantees that the results we show are ESS and not the result of drift, for instance, which will dominate for sections of the reaction norm that correspond to prevalences which have never occurred during a given simulation. The lines represent the median dispersal probability corresponding to that prevalence and the shaded regions are the quartiles. The panel is empty, the parasite went extinct in a majority of replicates before the end of the simulations runs. Constant model parameters:  $\lambda_0 = 4$ ,  $\alpha = 0.01$ ,  $\beta = 4$ ,  $a = 0.01$ ,  $\epsilon = 0.05$ . All simulations were run for 10000 time steps and analyses are executed on 10 replicate simulation runs.

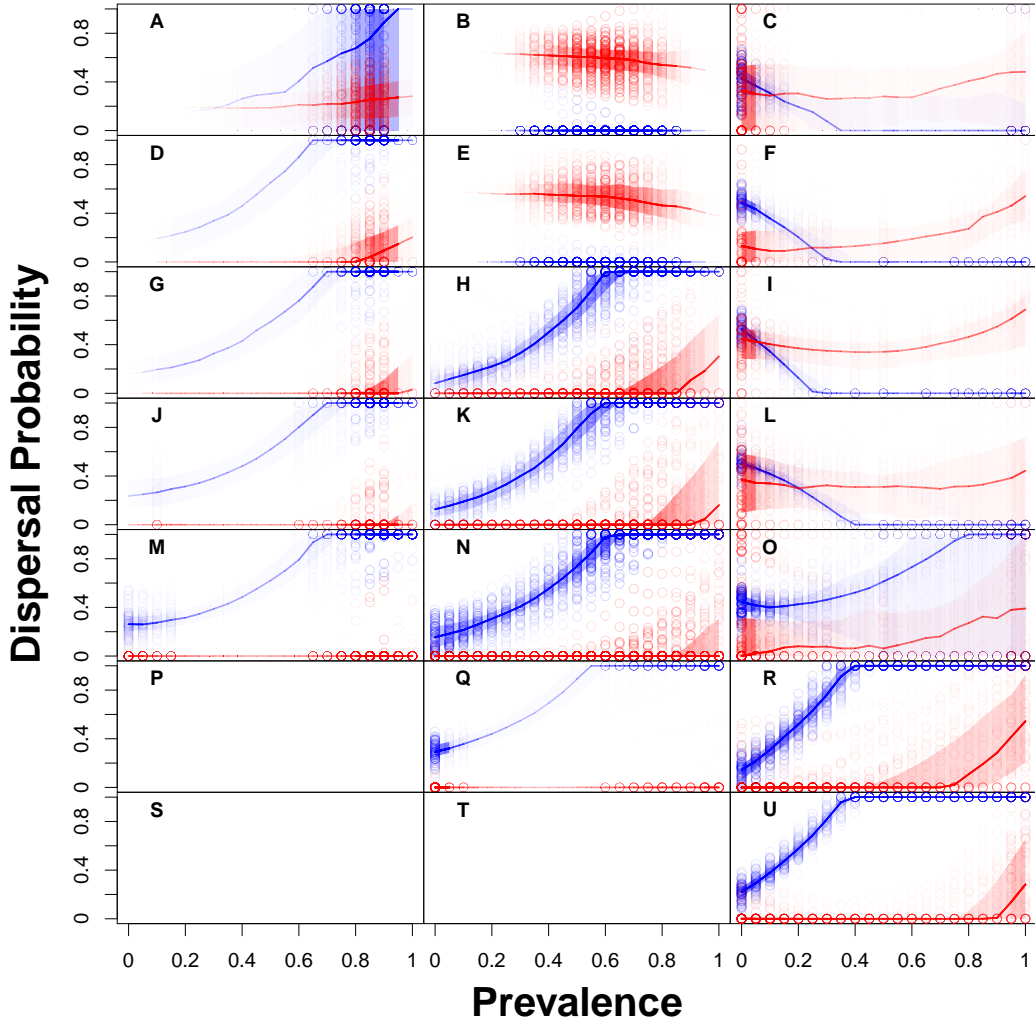


Figure S10: Evolutionarily stable dispersal reaction norms for prevalence- and infection state-dependent dispersal for differential dispersal costs of susceptible ( $\mu_{\text{susceptible}} = \text{const.} = 0.1$ ) and infected individuals (from top to bottom:  $\mu_{\text{infected}} = \{0.1, 0.12, 0.14, 0.16, 0.2, 0.3, 0.4\}$ ) when prevalences are shuffled in the landscape, which implies that kin competition is maintained but kin infection is statistically prevented. Red colours represent reaction norms of infected individuals and blue colours show reaction norms when susceptible. Virulence increases from left to right.  $v = 0.2$  for A, D, G, J and M,  $v = 0.5$  for B, E, H, K and N, and  $v = 0.8$  for C, F, I, L and O. This graph shows the reaction norms of 100 randomly chosen individuals at the end of the simulation (points) weighted by the normalised frequency of prevalences across space and time, that is, darker shades correspond to higher frequency of prevalence and lighter to lower frequency across space and time. We chose this weighting because the ecological settings of the simulations dictate the prevalences that occur and therefore also whether selection can act on parts of the reaction norm. Our approach (weighting combined with total simulation time, see Fig. S8) therefore guarantees that the results we show are ESS and not the result of drift, for instance, which will dominate for sections of the reaction norm that correspond to prevalences which have never occurred during a given simulation. The lines represent the median dispersal probability corresponding to that prevalence and the shaded regions are the quartiles. The empty panel is where the parasite went extinct in a majority of replicates before the end of the simulations runs. Constant model parameters:  $\lambda_0 = 4$ ,  $\alpha = 0.01$ ,  $\beta = 4$ ,  $a = 0.01$ ,  $\epsilon = 0.05$ . All simulations were run for 10000 time steps and analyses are executed on 10 replicate simulation runs.

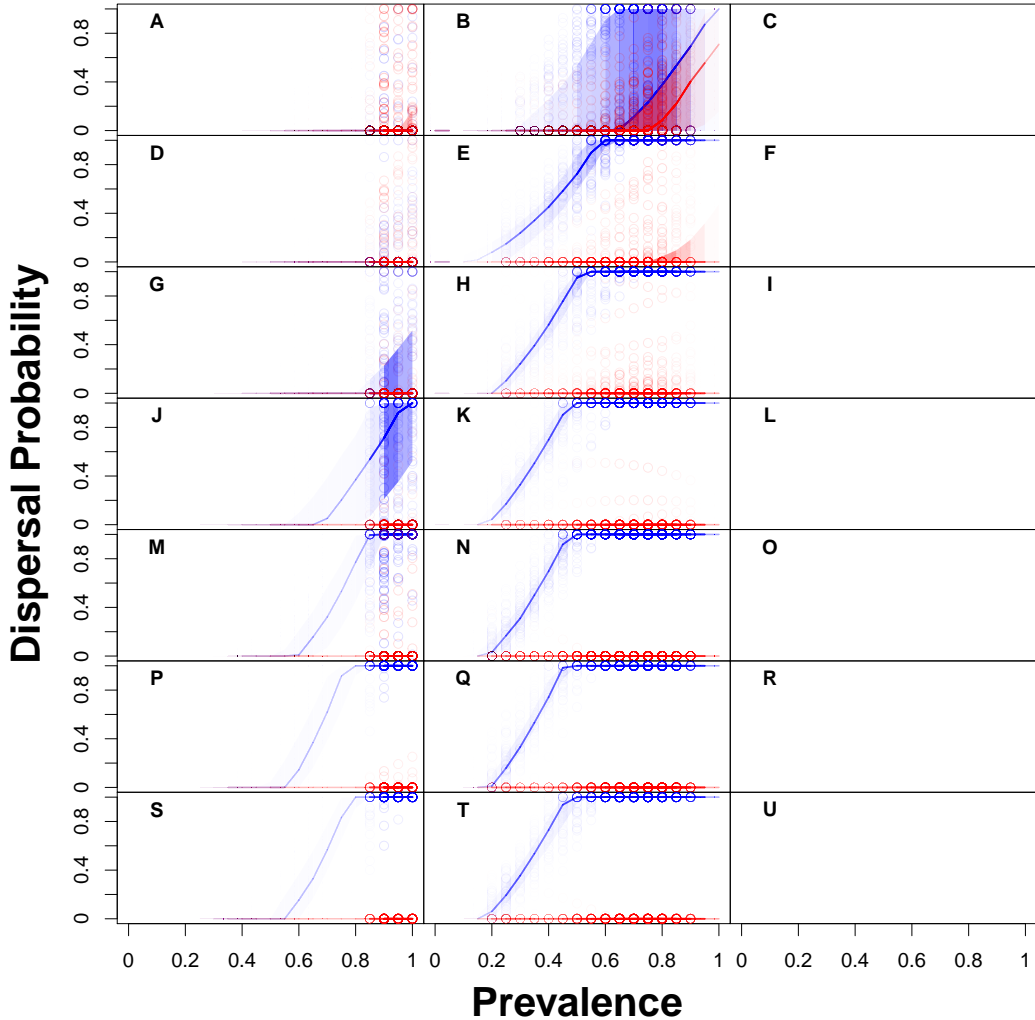


Figure S11: Evolutionarily stable dispersal reaction norms for prevalence- and infection state-dependent dispersal for differential dispersal costs of susceptible ( $\mu_{\text{susceptible}} = \text{const.} = 0.1$ ) and infected individuals (from top to bottom:  $\mu_{\text{infected}} = \{0.1, 0.12, 0.14, 0.16, 0.2, 0.3, 0.4\}$ ) when individuals are shuffled in the landscape, which implies that kin competition and kin infection are prevented. Red colours represent reaction norms of infected individuals and blue colours show reaction norms when susceptible. Virulence increases from left to right.  $v = 0.2$  for A, D, G, J and M,  $v = 0.5$  for B, E, H, K and N, and  $v = 0.8$  for C, F, I, L and O. This graph shows the reaction norms of 100 randomly chosen individuals at the end of the simulation (points) weighted by the normalised frequency of prevalences across space and time, that is, darker shades correspond to higher frequency of prevalence and lighter to lower frequency across space and time. We chose this weighting because the ecological settings of the simulations dictate the prevalences that occur and therefore also whether selection can act on parts of the reaction norm. Our approach (weighting combined with total simulation time, see Fig. S8) therefore guarantees that the results we show are ESS and not the result of drift, for instance, which will dominate for sections of the reaction norm that correspond to prevalences which have never occurred during a given simulation. The lines represent the median dispersal probability corresponding to that prevalence and the shaded regions are the quartiles. The empty panel is C, the parasite went extinct in a majority of replicates before the end of the simulations runs. Constant model parameters:  $\lambda_0 = 4$ ,  $\alpha = 0.01$ ,  $\beta = 4$ ,  $a = 0.01$ ,  $\epsilon = 0.05$ . All simulations were run for 10000 time steps and analyses are executed on 10 replicate simulation runs.

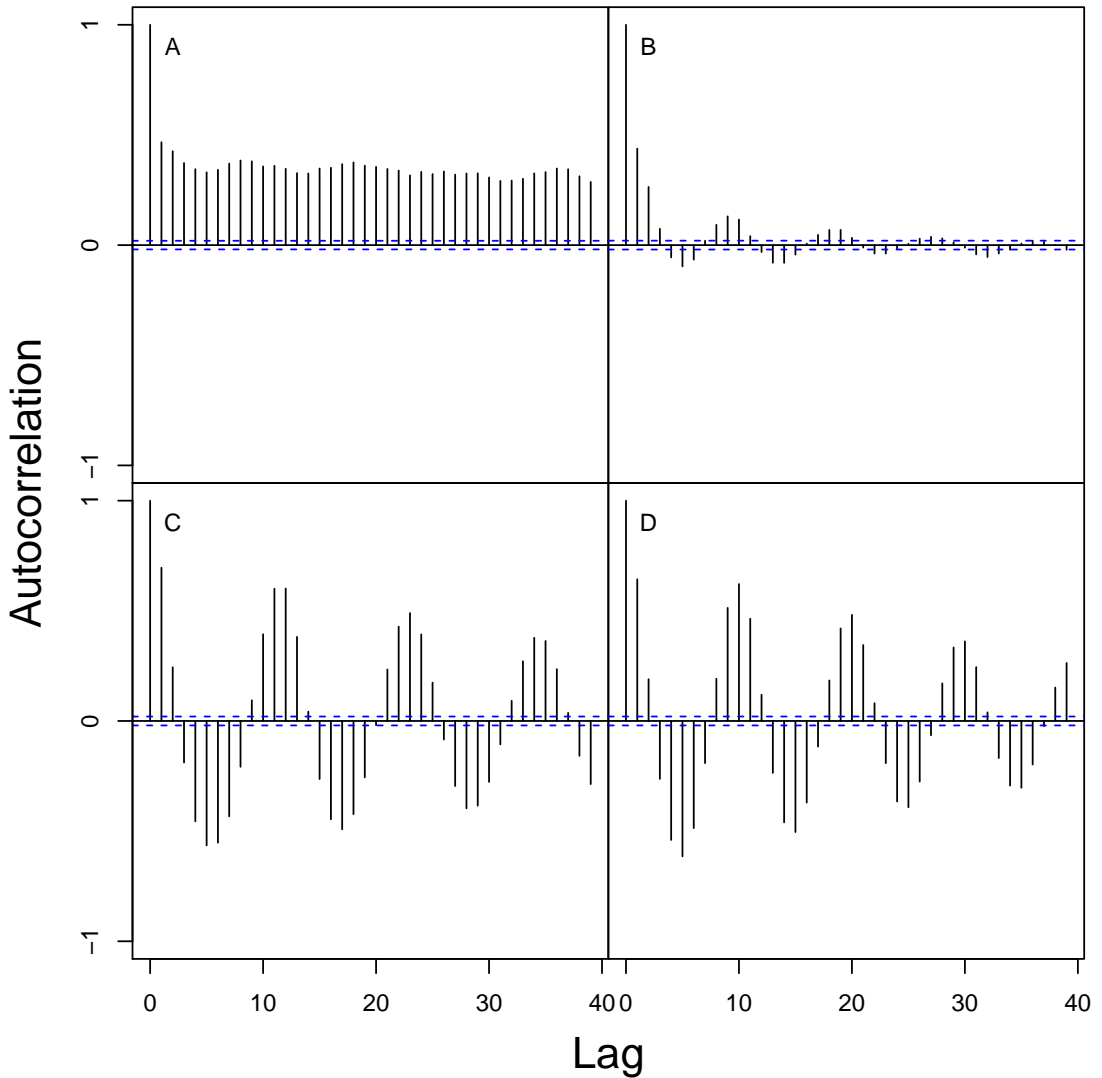


Figure A12. Autocorrelation of prevalences for the high virulence case, for different searching efficiency ( $a = 0.005, 0.01$  from left to right, and external extinction risk  $\varepsilon = 0, 0.05$ ).  $\lambda_0 = 4, \beta = 4, \mu = 0.1, v = 0.8$ ). Context-dependency evolves in the cases where there are oscillations (**B,C,D**), and does not evolve when the oscillations are absent (**A**).

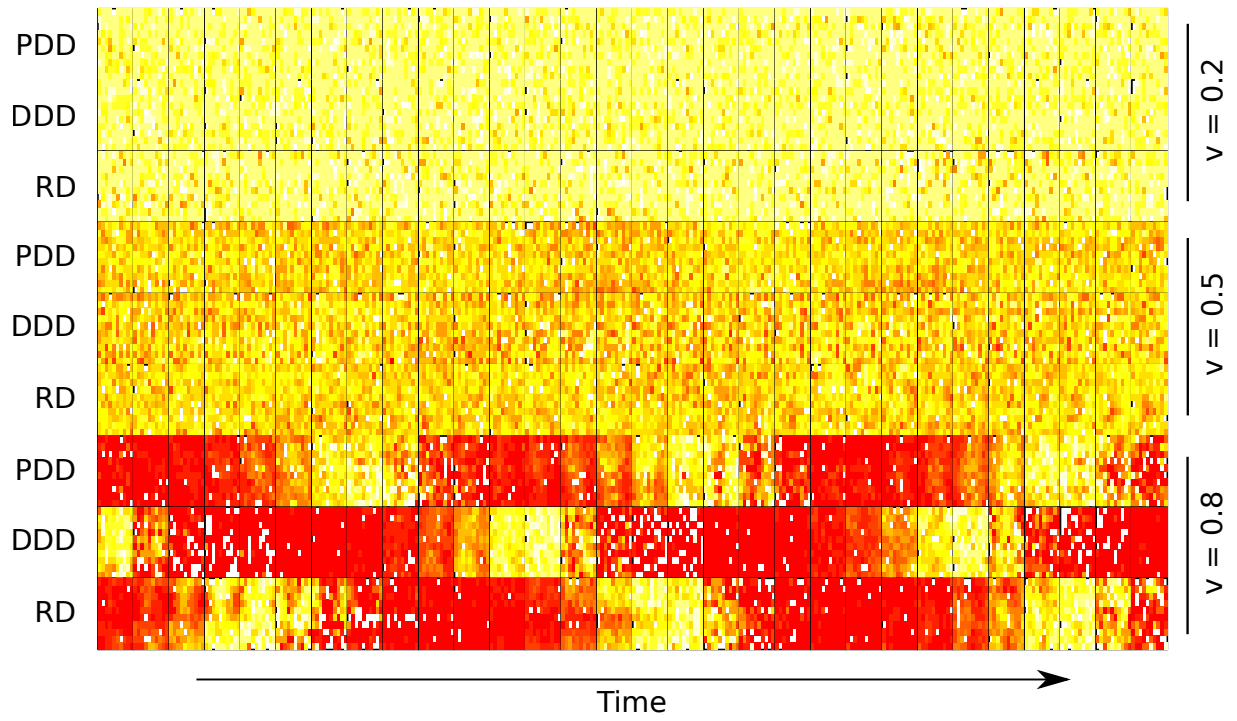


Figure A13. This figure shows the prevalence in each landscape for the last thirty time steps (from left to right). From top to down: the prevalence-dependent (PDD), density-dependent (DDD) and ecological scenarios (RD) are represented one after the other, for  $v = 0.2, 0.5, 0.8$  for the focal scenario ( $\lambda_0 = 4$ ,  $\beta = 4$ ,  $\mu = 0.1$ , and  $\varepsilon = 0.05$ ,  $a = 0.01$ ).

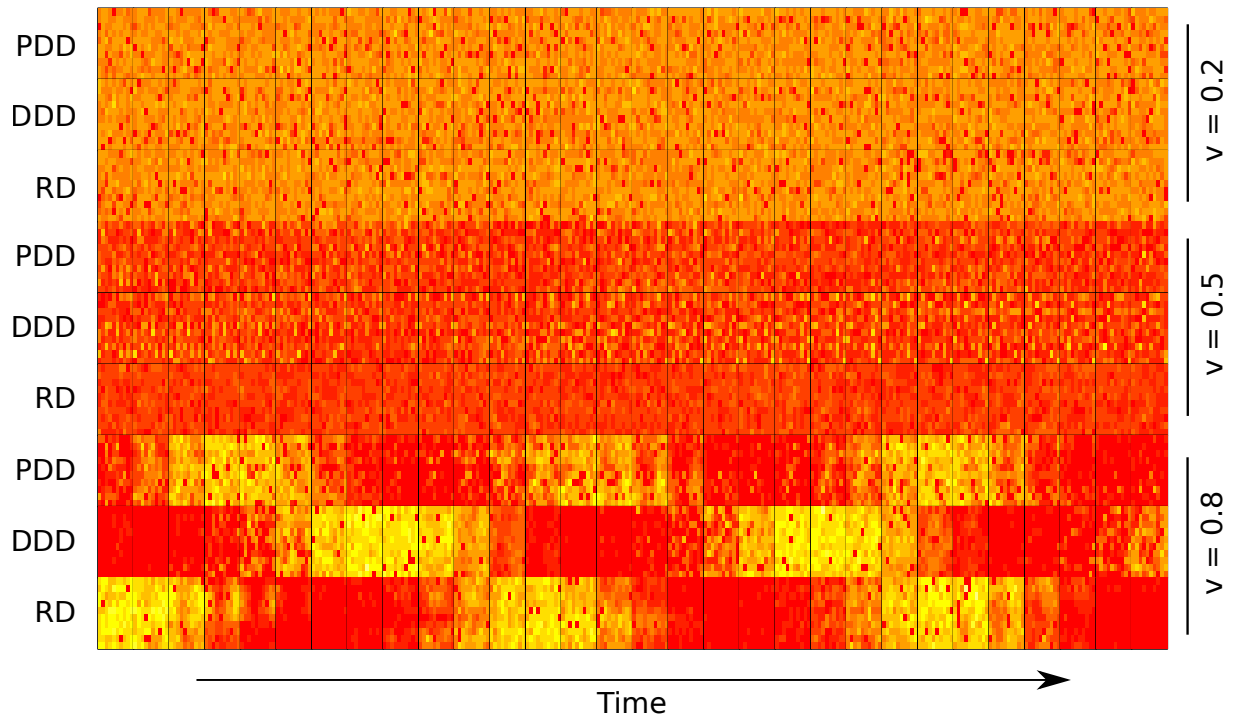


Figure A14. This figure shows the density in each landscape for the last thirty time steps (from left to right). From top to down: the prevalence-dependent (PDD), density-dependent (DDD) and ecological scenarios (RD) are represented one after the other, for  $v = 0.2, 0.5, 0.8$ , for the focal scenario ( $\lambda_0 = 4, \beta = 4, \mu = 0.1$ , and  $\varepsilon = 0.05, a = 0.01$ ).